

Single file and normal dual mode diffusion in highly confined hard sphere mixtures under flow.

Surajith N. Wanasundara,¹ Raymond J. Spiteri,² and Richard K. Bowles^{1, a)}

¹⁾*Department of Chemistry, University of Saskatchewan, Saskatoon, SK, S7N 5C9, Canada*

²⁾*Department of Computer Science, University of Saskatchewan, Saskatoon, SK, S7N 5C9, Canada*

(Dated: 19 August 2012)

We use Monte Carlo simulations to study the dual-mode diffusion regime of binary and tertiary mixtures of hard spheres confined in narrow cylindrical pores under the influence of an imposed flow. The flow is introduced to the dynamics by adding a small bias directed along the long axis of the pore to the random displacement of each Monte Carlo move. As a result, the motion of the particles in all the components is dominated by a drift velocity that causes the mean squared displacements to increase quadratically in the long time limit. However, an analysis of the mean squared displacements at intermediate time scales shows that components of the mixture above and below their passing thresholds still exhibit behaviors consistent with normal and single-file diffusion, respectively. The difference between the mean squared displacements of the various components is shown to go through a maximum, suggesting there may be an optimal pore diameter for the separation of mixtures exhibiting dual-mode diffusion.

^{a)}Electronic mail: richard.bowles@usask.ca

I. INTRODUCTION

The diffusion of fluids in highly confined geometries is important to a number of biological processes, such as the transportation of materials through ion channels, and engineering problems including the development of micro- and nano-fluidic devices. As a result, there has been considerable experimental and theoretical interest in understanding how particles move through narrow channels and pores.¹⁻⁶

For bulk fluids, the mean squared displacement (MSD) of the particles in the long time limit is given by the Einstein relation,

$$\langle \Delta x^2(t) \rangle = \langle (x(t) - x(0))^2 \rangle = 2D_x t , \quad (1)$$

where the average, $\langle \cdot \rangle$, is taken over the particles and D_x is the diffusion coefficient along an arbitrarily chosen axial x -direction. When the particles are confined to channels so narrow that they are unable to pass each other, the geometric constraints restrict the particles to a single file and the nature of the dynamics can change. If the confined particles are subjected to a deterministic dynamics, such as in molecular dynamics, the MSD continues to follow Eq. (1). However, if the confined particles are subject to a Brownian background,⁷ like confined colloids suspended in a supporting fluid⁸⁻¹⁰ or independent stochastic forces,¹¹ then the MSD becomes proportional to $t^{1/2}$ and is described by an Einstein-like relation

$$\langle \Delta x^2(t) \rangle = 2F_x t^{1/2} , \quad (2)$$

where the mobility factor F replaces the diffusion coefficient. This is known as *single-file diffusion* (SFD) or anomalous diffusion and is the focus of the current work.

A dynamic transition from anomalous SFD to normal diffusion has been observed in single-file Lennard–Jones¹² and hard sphere¹³ particles when the pore diameter is increased beyond the passing threshold, which represents the diameter where particles are just able to pass each other. One approach to understanding the nature of the dynamics in this transition regime is to focus on the hopping time, τ_{hop} , which measures the average time it takes for a particle to escape the cage formed by its two neighbors.¹³⁻¹⁶ For times less than τ_{hop} , the particles remain trapped between their neighbors and perform SFD, but because they eventually pass, the diffusion crosses over to normal diffusion in the long time limit. In this case, $D_x \sim \tau_{hop}^{-1/2}$.¹³ The hopping time itself has been found to behave as a power law

in the reduced pore diameter, which measures the space available for particles to pass, and diverges as the pore diameter approaches the passing threshold from above. As a result, the diffusion coefficient and hopping time are highly sensitive to the diameter of the pore.

The separation of microparticles based on size is an important process for many medicinal, biological, and industrial applications, such as drug delivery^{17,18} and clinical analysis,^{19,20} with the most significant challenge being the separation of particles with a narrow size distribution. If a binary mixture of particles with different sizes is confined to a quasi-one-dimensional pore, then it is possible to establish a regime of dual-mode diffusion, where one component is below its passing threshold and exhibits SFD while the other component is able to pass its neighbors and performs normal diffusion.^{1,3,21,22} The hopping time is highly sensitive to the reduced pore diameter, thus opening up the possibility of using dual-mode diffusion to separate particles that are only marginally different in size. However, in order to perform a separation based on dual-mode diffusion, it is necessary to drive the mixture through the pore with an imposed flow. The goal of the present work is to examine the effects of an imposed flow on the diffusive properties of highly confined hard sphere mixtures in a cylindrical pore and to demonstrate that dual-mode diffusion persists in presence of a drift velocity. The remainder of the paper is organized as follows: Section II describes the methods. Section III contains our results and discussion. Section IV contains our conclusions.

II. METHODS

We study equimolar binary and tertiary mixtures of three-dimensional hard spheres confined to long, narrow, structureless cylindrical pores with hard walls. Component i of the mixtures consists of M_k spheres of diameter σ_k . For simplicity, we use the size of the largest particles as the unit of length. We also focus on a binary mixture with $\sigma_2/\sigma_1 = 0.8$ while the tertiary mixture contains particles with $\sigma_2/\sigma_1 = 0.9$ and $\sigma_3/\sigma_1 = 0.8$, unless stated otherwise. Two particles of species k and l respectively, interact with a potential energy defined by

$$V(r) = \begin{cases} 0 & \text{if } r \geq \sigma_{kl}, \\ \infty & \text{if } r < \sigma_{kl}, \end{cases}$$

where r is the distance between the particles and $\sigma_{kl} = (\sigma_k + \sigma_l)/2$.

The particles are confined to a quasi-one-dimensional cylindrical pore that has the long axis extending in the x -direction. Particles of species k interact with the walls with a potential energy,

$$V_W(h) = \begin{cases} 0 & \text{if } h \leq R_k, \\ \infty & \text{if } h > R_k, \end{cases}$$

where h is the absolute distance between the center of the particle and the center axis of the channel in the yz plane, $R_k = (D_p - \sigma_k)/2$, and D_p is the diameter of the pore. The pore is considered to be infinitely long in both the positive and negative x -directions and no periodic boundaries are applied. Initially, the particles are randomly distributed within a region of the tube of length L so that the linear density of the starting configuration $\phi_L = \sum_k M_k \sigma_k / L = 0.5$ and the components of the mixtures are uniformly mixed.

One of the main advantages of studying the hard sphere system is that the passing threshold, which represents the pore diameter at which two particles of species k and l can just pass each other, can be rigorously defined as $\Delta_{kl}^* = (\sigma_k + \sigma_l)$ because the interaction potential becomes infinite if there is a particle-particle or particle-wall overlap. For the binary mixture, $\Delta_{11}^* = 2.0$, $\Delta_{12}^* = 1.8$, and $\Delta_{22}^* = 1.6$. However, it is important to note that once the pore diameter is below Δ_{12}^* , the system remains in a single file even though the small particles can pass each other because the small particles are still trapped in cages formed by the large particles. Similarly, the passing thresholds in the three-component system are $\Delta_{11}^* = 2.0$, $\Delta_{12}^* = 1.9$, $\Delta_{22}^* = \Delta_{13}^* = 1.8$, $\Delta_{23}^* = 1.7$, and $\Delta_{33}^* = 1.6$.

The presence of a random element in the particle dynamics is essential to the SFD phenomenon because without it the particles always exhibit normal diffusion. We move the particles using the standard Metropolis Monte Carlo (MC) algorithm²³ as a simple approximation to Brownian motion in a hard particle system. A particle is selected at random and moved a small **fixed distance, $\delta\mathbf{r}$** , in a randomly selected direction. If the new position of the particle places some or all of it outside the pore or causes an overlap with another particle, the move is rejected and the particle returned to its original position. Otherwise, the particle move is accepted. This procedure is repeated N times in a single MC cycle and we use one MC cycle as our unit of time. To simulate the effect of an imposed flow in our system, we add a small bias $\delta x = 2 \times 10^{-5}$ to the x -component of $\delta\mathbf{r}$ and renormalize the vector so the total ~~step length~~ remains the same.

The motion of the particles during the simulation is characterized by following the MSD

as a function of time,

$$\text{MSD} = \langle \Delta r^2(t) \rangle = \frac{1}{N} \sum_{i=1}^N (\mathbf{r}_i(t) - \mathbf{r}_i(0))^2, \quad (3)$$

where $\mathbf{r}_i(0)$ and $\mathbf{r}_i(t)$ are the positions of particle i at the time origin and a later time, t , respectively. The mean squared displacement for the different components, MSD_k , is obtained by simply restricting the average in Eq. (3) to the particles of species k . Simulations are performed on pores with diameters ranging from 1.79 to 5.00 and each simulation is run for 5.0×10^8 MC cycles.

III. RESULTS AND DISCUSSION

In the absence of any bias, the general form of the MSD for each species measured in our simulation is the same as that measured in equilibrium.³ With $D_p < \Delta_{12}^*$, the $\text{MSD} \sim t^{1/2}$ at intermediate and long times. Increasing D_p above Δ_{12}^* allows the small particles to pass and they exhibit normal diffusion while the large particles continue to diffuse anomalously, giving rise to the dual-mode diffusion phenomenon, until the pore diameter is above Δ_{11}^* , at which point the $\text{MSD} \sim t$ for both components in the long time limit.

Figure 1 shows that at intermediate times the MSDs of the two particle sizes under a small bias remain the same as in the unbiased case. In the pore with ~~diameter~~ 1.79, the MSDs of both the small and large particles increase linearly as a function of $t^{1/2}$ (Figure 1(a)), suggesting both components exhibit SFD. Although $D_p = 1.79$ is wide enough to allow the small particles to pass each other, it is below Δ_{12}^* . As a result, the small particles are permanently caged by large particles and the large particles are trapped in cages formed by both small and large particles. With ~~a pore diameter~~ 1.99, Figure 1(b) shows that the MSD of the small particles increases linearly as a function of t , but the MSD of the large particles increases linearly as function of $t^{1/2}$, indicating that small particles undergo normal diffusion whereas large particles still exhibit SFD. Here, the small particles can now pass the large particles and the large particles remain caged.

When the pore diameter is increased above the passing threshold for the large particles, the MSD of both components becomes linear in t . However, the diffusion coefficients for the two components are different when $D_p = 2.20$ (Fig 1(c)), and they are the same when $D_p = 5.00$ (Fig 1(d)). To understand this, we note that in the crossover region between

anomalous and normal diffusion, particles are caged for long periods of time before they actually hop past their neighboring particle simply because the space available for two particles to pass is still small. While a particle is caged, it behaves as if it is in a single file and its MSD increases as $t^{1/2}$, but it eventually passes and we see normal diffusion on time scales longer than the average hopping time. In this regime, the diffusion coefficient goes as $\tau_{hop}^{-1/2}$, where τ_{hop} is the average hopping time. The hopping times themselves are power laws in the space available for passing, suggesting that the diffusion coefficient is sensitive to the pore diameter. We see this effect clearly when $D_p = 2.20$ because the hopping time for the large particles is still expected to be long compared to that of the small particles. By the time the pore diameter reaches 5.00, all the particles pass each other easily, suggesting we have reached the bulk regime, where single file caging is no longer relevant, and we see both types of particles diffusing at the same rate. This effect is observed even in the absence of a bias.

Figure 2 shows the MSDs of the two particle sizes in the binary mixture as a function of time, t , for pore diameters of 1.79, 1.99, 2.20, and 5.00 in the presence of bias over long times. We now see a crossover to a new behavior where the MSDs increase as t^2 . Simulation studies of ions in a bulk fluid moving under the influence of an external field^{24,25} and experiments following nanoparticle tracers flowing through the tail veins of mice²⁶ also report that the biased motion of particles with a drift velocity causes the MSD to increase proportionally with t^2 . Even though the bias in our simulations is small, the t^2 term dominates in the calculated MSD in the long time limit, but it is important to note that the introduction of the drift velocity does not appear to destroy the SFD and dual-mode diffusion phenomena. For each D_p , we followed the MSD using two independent time origins, selected as $t = 2.0 \times 10^8$ and $t = 4.0 \times 10^8$ after the simulation had started, and found that the intermediate time behavior is recovered in both cases.

In the context of separating mixtures, the difference in MSDs, $\Delta\text{MSD}_{21} = \text{MSD}_2 - \text{MSD}_1$ is the quantity of most interest. In addition, if the drift velocity caused by the bias affects both particles equally, the t^2 term cancels out to reveal what could be considered to be the intrinsic diffusive properties of the particles. Figure 3 shows that ΔMSD_{21} is linear in t for all pore diameters, except when $D_p = 1.79$ and 5.00. When ~~the pore diameter is above~~ Δ_{11}^* , both particle types can pass and the two components diffuse normally. On the basis of Eq. (1), we might expect a linear dependence of ΔMSD_{21} . However, below the passing

threshold of the large particles, ΔMSD_{21} has a form given by the difference of Eqs. 1 and 2, but we only see the linear term in Figure 3 because this only dominates at longer times.

It is evident from Figure 3 that the slopes of ΔMSD_{21} are a non-monotonic function of the pore diameter and the relative mobilities of the particles at a fixed time go through a maximum. This suggests that there is an optimal pore diameter for maximizing the difference in mobilities of the different components, likely leading to improved separation. In order to locate this optimal pore diameter, the MSDs for the particles are calculated at intervals of $\Delta t = 1.0 \times 10^6$. Using a number of time points along the trajectory as independent time origins to improve the statistical properties of the measurements, the MSD is calculated to give $\langle \Delta\text{MSD}_{21} \rangle$ (Figure 4). The most obvious feature is the presence of the maximum at $D_p \approx 2.06$. In the range of pore diameters, $\Delta_{12}^* \leq D_p \leq \Delta_{11}^*$, $\langle \Delta\text{MSD}_{21} \rangle$ increases because the small species diffuses normally and the large particles diffuse anomalously. Once D_p is above the passing threshold for the large particles, both components diffuse normally, but we expect $\langle \Delta\text{MSD}_{21} \rangle$ to continue to increase because the hopping times for the large particles are still long compared to those of the small particles. However, eventually the pore becomes so wide that the single file description no longer applies. Both components then diffuse at the same rate and $\langle \Delta\text{MSD}_{21} \rangle$ tends to zero. This suggests that $\langle \Delta\text{MSD}_{21} \rangle$ should exhibit a maximum, but whether the crossover to purely bulk behavior occurs at sufficiently narrow pore diameters to explain the location of the maximum observed in Figure 4 is not clear. Repeating the simulations for different biases, $\delta x = 0, 2.0 \times 10^{-5}$ and 5.0×10^{-5} , shows that the position of the maximum is independent of the bias and that our expectation that the drift velocity affects each component equally so that it cancels out in ΔMSD_{21} is justified, at least for the pore sizes near the maximum. We see some small deviations between the simulations at different degrees of bias at larger pore sizes.

The three-component system exhibits the same general features as the binary mixture. Figure 5 shows $\langle \Delta\text{MSD}_{kl}^{(3)} \rangle$ for each of the possible pairs of components in the ternary mixture. These are also compared to $\langle \Delta\text{MSD}_{kl}^{(2)} \rangle$ for binary mixtures that have σ_k/σ_1 and σ_l/σ_1 as the ternary mixture. The **super scripts**, (2) and (3), denote the number of components. We find that the mobility of the two smallest components, relative to the largest, is the same in both the two- and three-component systems, but the difference between the MSDs of the small components in the ternary mixture, with $\sigma_2 = 0.9$ and $\sigma_3 = 0.8$ is not the same in the binary mixture containing the same two components. This demonstrates that

it is the ability of a given sized particle to hop past the largest particles in the system that ultimately controls the nature of the diffusion in this dual-mode regime because it is the largest particles that determine the passing threshold for each component's transition from single-file to normal diffusion.

In order to demonstrate that the general features of SFD and dual-mode diffusion persist in the presence of a flow that generates a drift velocity, we have focused our attention on measurements of the MSD of particles subjected to a small bias. Increasing the bias causes the t^2 term to dominate at earlier times, thus swamping the signatures of the SFD. As a result, we do not directly observe the separation of the mixtures on the time scale of our simulations. The difference in mobilities of the components along the tube is a prerequisite for separation, but it still remains to be demonstrated that the conditions that maximize $\langle \Delta \text{MSD}_{21} \rangle$ result in the optimal separation of mixtures exhibiting dual-mode diffusion.

IV. CONCLUSIONS

The primary goal of this work was to explore the effects of flow on the diffusive properties of hard sphere particles confined to narrow pores where we observe dual-mode diffusion. The addition of a directional bias to the dynamics dramatically changes the general functional form of the diffusion at long times but our analysis of the MSDs over intermediate timescales shows that the characteristic behaviors of the single-file and normal diffusion components remain the same. Furthermore, our work highlights the ability of single-file confinement to enhance the difference in mobility of two components of a mixture that are highly similar in size.

ACKNOWLEDGMENTS

This work was supported by the Natural Sciences and Engineering Research Council of Canada through the Discovery and Engage Grants programs and by POS Bio-Sciences. All computations were performed using computing resources provided by WestGrid (www.westgrid.ca) and Compute/Calcul Canada.

REFERENCES

- ¹P. Adhangale and D. Keffer, *Mol. Phys.* **100**, 2727 (2002).
- ²S. R. Majumder, N. Choudhury, and S. K. Ghosh, *J. Chem. Phys.* **127**, 054706 (2007).
- ³C. D. Ball, N. D. MacWilliam, J. K. Percus, and R. K. Bowles, *J. Chem. Phys.* **130**, 054504 (2009).
- ⁴J. B. Delfau, C. Coste, C. Even, and M. Saint Jean, *Phys. Rev. E* **82**, 031201 (2010).
- ⁵S. Y. Yang, J.-A. Yang, E.-S. Kim, G. Jeon, E. J. Oh, K. Y. Choi, S. K. Hahn, and J. K. Kim, *ACS Nano*. **4**, 3817 (2010).
- ⁶B. Mukherjee, P. K. Maiti, C. Dasgupta, and A. K. Sood, *ACS Nano*. **4**, 985 (2010).
- ⁷D. G. Levitt, *Phys. Rev. A* **8**, 3050 (1973).
- ⁸Q.-H. Wei, C. Bechinger, and P. Leiderer, *Science* **287**, 625 (2000).
- ⁹C. Lutz, M. Kollmann, and C. Bechinger, *Phys. Rev. Lett.* **93**, 026001 (2004).
- ¹⁰B. Lin, M. Meron, B. Cui, S. A. Rice, and H. Diamant, *Phys. Rev. Lett.* **94**, 216001 (2005).
- ¹¹J. K. Percus, *Phys. Rev. A* **9**, 557 (1974).
- ¹²K. Hahn and J. Kärger, *J. Phys. Chem. B* **102**, 5766 (1998).
- ¹³K. K. Mon and J. K. Percus, *J. Chem. Phys.* **117**, 2289 (2002).
- ¹⁴R. K. Bowles, K. K. Mon and J. K. Percus, *J. Chem. Phys.* **121**, 10668 (2004).
- ¹⁵K. K. Mon and J. K. Percus, *J. Chem. Phys.* **127**, 094702 (2007).
- ¹⁶K. K. Mon, *J. Chem. Phys.* **130**, 184701 (2009).
- ¹⁷D. Di Carlo, D. Irimia, R. G. Tompkins, and M. Toner, *Proc. Natl. Acad. Sci. U.S.A.* **104**, 18892 (2007).
- ¹⁸G. Su and R. M. Pidaparti, *J. Nanotechnol. Eng. Med.* **2**, 021006 (2011).
- ¹⁹M. Toner and D. Irimia, *Annu. Rev. Biomed. Eng.* **7**, 77 (2005).
- ²⁰A.-E. Saliba, L. Saias, E. Psychari, N. Minc, D. Simon, F.-C. Bidard, C. Mathiot, J.-Y. Pierga, V. Fraissier, J. Salamero, V. Saada, F. Farace, P. Vielh, L. Malaquin, and J.-L. Viovy, *Proc. Natl. Acad. Sci. U. S. A.* **107**, 14524 (2010).
- ²¹D. S. Sholl and K. A. Fichthorn, *J. Chem. Phys.* **107**, 4384 (1997).
- ²²P. Adhangale and D. Keffer, *Sep. Sci. Technol.* **38**, 977 (2003).
- ²³D. Frenkel and B. Smit, editors, *Understanding Molecular Simulation: From Algorithms to Applications*, Academic Press, New York, 2002.
- ²⁴S. H. Lee and J. C. Rasaiah, *J. Chem. Phys.* **101** 6964 (1994).

²⁵S. Murad, J. Chem. Phys. **134**, 114504 (2011).

²⁶M. Kawai, H. Higuchi, M. Takeda, Y. Kobayashi, and N. Ohuchi, Breast Cancer Res. **11**, R43 (2009).

Captions

Fig. 1. The MSDs for the components of the binary mixture as a function of time at intermediate timescales for pore sizes (a) 1.79, (b) 1.99, (c) 2.20, and (d) 5.00. The solid and dashed lines represent the large and small particles respectively. The dashed triangles indicate line slopes for comparison.

Fig. 2. The MSDs of the large (solid lines) and small (dashed lines) particles in the binary mixture as a function of time for pore diameters, D_p , (a) 1.79, (b) 1.99, (c) 2.20, and (d) 5.00 at long times. The dashed triangles indicate line slopes for comparison.

Fig. 3. ΔMSD_{21} for the binary mixture as a function of time for different pore diameters.

Fig. 4. $\langle\Delta\text{MSD}_{21}\rangle$ as a function of pore diameter for the binary mixture with no bias (circles), a bias of $\delta x = 2.0 \times 10^{-5}$ (squares) and a bias of $\delta x = 5.0 \times 10^{-5}$ (diamonds).

Fig. 5. $\langle\Delta\text{MSD}_{kl}^{(3)}\rangle$ for the ternary mixture and $\langle\Delta\text{MSD}_{kl}^{(2)}\rangle$ the corresponding binary mixtures as a function of pore diameter.

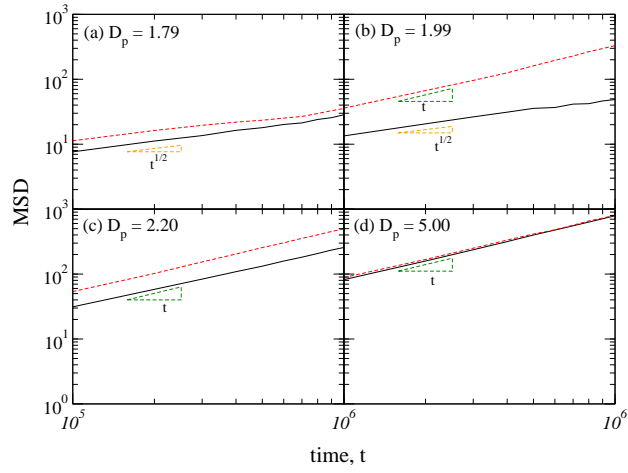


FIG. 1. The MSDs for the components of the binary mixture as a function of time at intermediate timescales for pore sizes (a) 1.79, (b) 1.99, (c) 2.20, and (d) 5.00. The solid and dashed lines represent the large and small particles respectively. The dashed triangles indicate line slopes for comparison.

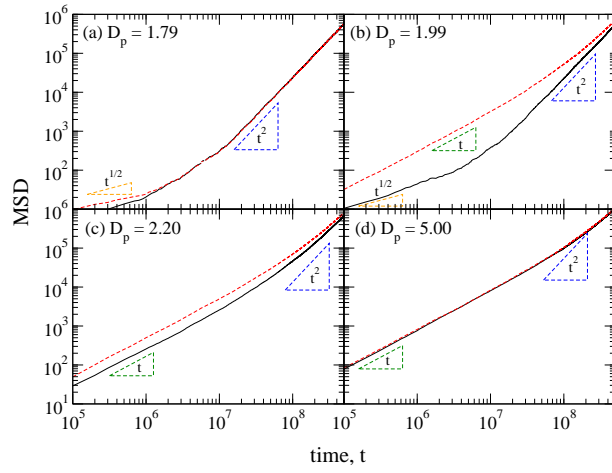


FIG. 2. The MSDs of the large (solid lines) and small (dashed lines) particles in the binary mixture as a function of time for pore diameters, D_p , (a) 1.79, (b) 1.99, (c) 2.20, and (d) 5.00. The dashed triangles indicate line slopes for comparison.

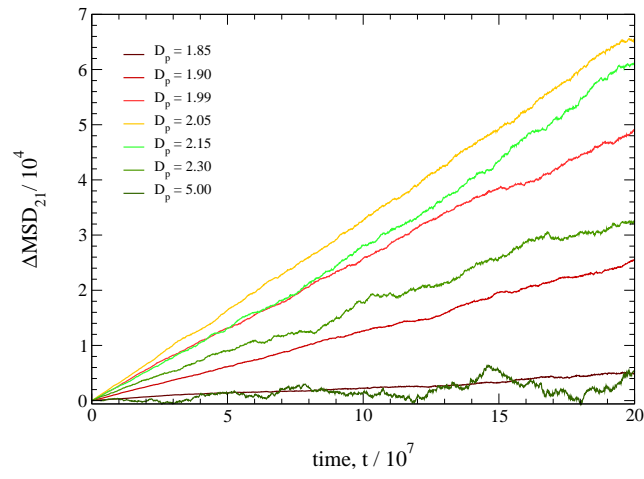


FIG. 3. ΔMSD_{21} for the binary mixture as a function of time for different pore diameters.

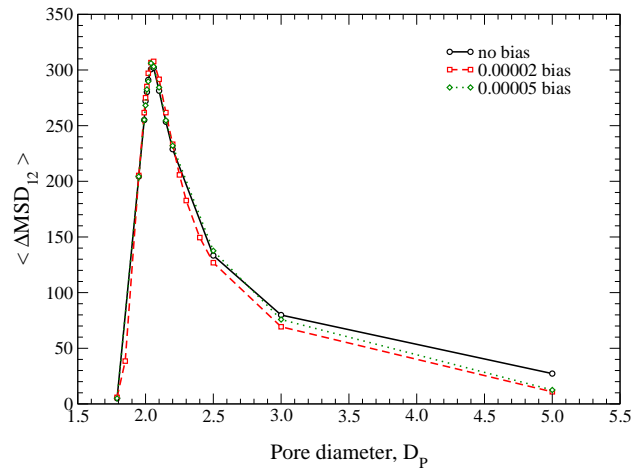


FIG. 4. $\langle \Delta \text{MSD}_{21} \rangle$ as a function of pore diameter for the binary mixture with no bias (circles), a bias of $\delta x = 2.0 \times 10^{-5}$ (squares), and a bias of $\delta x = 5.0 \times 10^{-5}$ (diamonds).

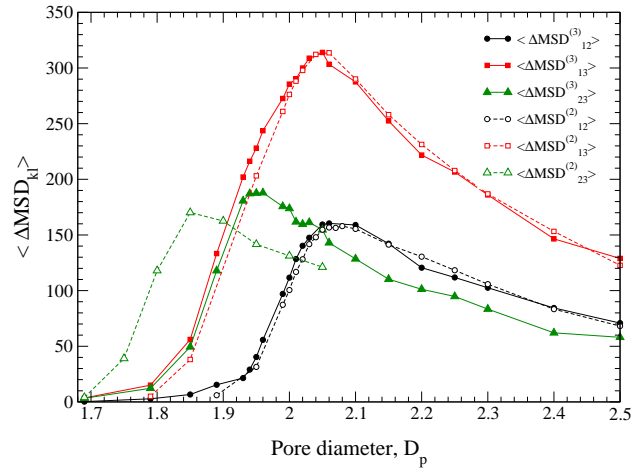


FIG. 5. $\langle \Delta MSD_{kl}^{(3)} \rangle$ for the ternary mixture and $\langle \Delta MSD_{kl}^{(2)} \rangle$ the corresponding binary mixtures as a function of pore diameter.